Project Title: Room Temperature Electrochemical Upgrading of Methane to Oxygenate Fuels

DOE Grant Number: **DE-SC0010531**

PI: **William E. Mustain**
Position Title of PI: **Associate Professor**
Affiliation: **University of Connecticut**
Department of Chemical and Biomolecular Engineering
Mailing Address of PI: **191 Auditorium Rd**
Unit 3222
Storrs, CT 06269-3222
Telephone Number of PI: **860-486-2756**
Email of PI: **mustain@engr.uconn.edu**

Graduate Students: **Neil Spinner, Travis Omasta, Xiong Peng, Shuai Zhao**
Undergraduates: **Derek Chhiv, Connor Lewis**
Total Budget: **$640,000**
Project Period: **09/01/2013-08/31/2017**

Technical Abstract

The overall objective of this project is to discover the nature of the electrochemically active sites and to uncover the mechanisms for the electrocatalytic transformation of small organic molecules to oxygenate products such as methanol, formaldehyde, carbon monoxide and acetylene. Among the feedstocks of interest in this study are: methane, carbon dioxide, and acetic acid. Methane is an incredibly attractive potential feedstock because of the recent discovery of large shale deposits; carbon dioxide is potentially a very available feedstock from carbon capture technologies; acetic acid (as well as CH_4 and CO_2 and ethanol) has potential as a bio-derived feedstock. This report summarizes the major results to date regarding the electrochemical transformation of CH_4, CO_2 and acetic acid to chemicals and fuels – with a primary focus on methane. Finer details are available in each of the projects annual reports. In addition to the primary objective, the work in this project has led to synergistic discoveries that are advantageous to other fields including: catalyst layer deposition, anion exchange membrane fuel cells, CO_2 capture and li-ion batteries. Those are very briefly discussed as well.

A. Motivation

There is no question that the energy landscape in the United States is undergoing a metamorphosis towards energy carriers and energy conversion processes that possess a reduced anthropogenic carbon footprint. Because of its increased efficiency compared to internal combustion, the transportation sector is seeing the gradual electrification of passenger vehicles which is expected to dramatically grow in the next decade [1-2]. In the electricity sector, coal is becoming less and less economically attractive and is being replaced largely by natural gas and an ever-increasing amount by solar and other renewable energy technologies that are becoming more and more cost competitive every day [3]. On top of this, the threat of global climate change has brought considerable social, economic and political attention to the need for a significant reduction in CO_2 emissions around the world [4-5]. However, in the industrial sector, the least efficient sector in our economy after transportation [6], transformative innovations have lagged. The largest subset of the industrial sector from an energy perspective is the production of commodity chemicals – accounting for 5.5% of global energy consumption [7-8], which relies heavily on conventional natural gas and petrochemical processing.

As the main component of natural gas, methane is a well-established and widely available (at low cost with the recent discoveries of vast amounts of shale gas) feedstock for the production of chemicals, particularly small chain organics, Figure 1a. Despite being widely deployed, its use has an intrinsic constraint that makes the process unavoidably expensive and environmentally concerning: methane is first converted to synthesis gas ("syngas") through steam reforming, which is done at very high temperatures (~ 900°C) and is very highly exothermic (ΔH_{900C} = 227 kJ/mol). The need for this significant amount of high-quality heat is met through burning of additional methane, making this process extremely carbon inefficient (~1/2 of all methane becomes CO_2, not a desired product). Therefore, many have called for the low temperature, direct transformation of methane to chemicals and fuels one of the "Holy Grails in Chemistry" [9-11] – and advances in catalysis are central to achieving it [12]

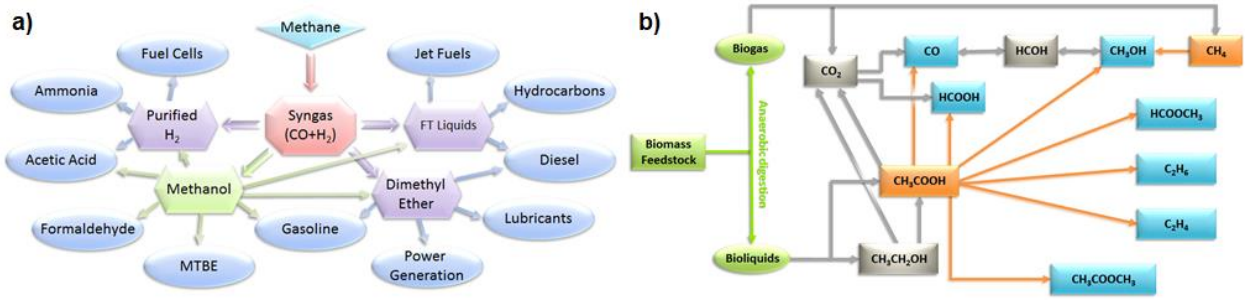

Figure 1. Chemical pathways for the production of fuels and chemicals from: a) conventional highly CO_2 emitting methane steam reforming; and b) biological feedstocks and fermentation products (based on preliminary data).

On the petrochemical side, refining provides two primary classes of intermediate chemicals in addition to syngas: olefins (e.g. ethylene) and aromatics (e.g. benzene), which are converted in downstream or off-site processes to commodity and specialty chemicals. Both olefins and aromatics are typically obtained from steam cracking of hydrocarbon feedstocks. Steam cracking requires a very large energy input – where the latent heat of water needs to be overcome

and the resulting vapor superheated to 850°C; in fact, in a typical petrochemical plant, steam cracking alone is responsible for more than 1/3 of the consumed energy [13]. The boiler requirements are met by burning natural gas and gas-phase refining products. Additionally, separations processes, pumps, compressors, etc. consume additional thermal and electrical energy. In the end, the combination of losses translates into very poor carbon efficiency for chemicals produced through petrochemical processing – where as little as 46% [13-14] of the C atoms that enter the facility may become desired products, and the rest are lost to the atmosphere as CO_2.

Therefore, there is a strong desire to replace these fossil fuel dependent processes with alternatives that have reduced energy consumption – particularly high temperature energy – as well as higher carbon efficiency and lower CO_2 emissions. One of the most promising alternatives, which has been discussed for several years, is biomass [14-16]. It has been estimated that if properly implemented biomass could account for 60% of all renewable energy use in only ~15 years [17]. Biomass has the distinct advantage of being able to sequester expended CO_2 at the rate it is evolved (unlike geological sources), assuming that it is replaced at the same rate it is consumed. Additionally, biomass can provide pathways to create complex organic molecules. Though there are many routes for the conversion of biological sources to fuels and chemicals (e.g. gasification), biomass fermentation (anaerobic digestion) is likely the most attractive due to its relatively low energy demand, low temperature operation, and product selectivity. Though there are many possible products that are possible from naturally-occurring and genetically modified species, four of the primary products from fermentation are: ***methane*** and ***CO_2*** gases, and ***ethanol*** and ***acetic acid*** liquids. Therefore, it is expected that these four molecules will be important feedstocks for next-generation processes and ***provide the building blocks to produce future fuels and chemicals***, as illustrated in Figure 2.

Further supporting the importance of studying these four molecules is: i) the explosion in the availability of low cost methane through the shale gas boom; ii) the likelihood for large volumes of CO_2 that are expected emerge as a feedstock resulting from the extensive global carbon capture efforts currently underway; and iii) the regional diversity of biomass [18-19] and need to have standardized ways to process their fermentation products. Hence, if the chemical industry is to move towards biological feedstocks, and pathways that consume the lowest amount of energy, the U.S. will likely see a regionalization of processing pathways [19] where the optimal path to produce methanol in Pennsylvania may be drastically different than North Dakota, which calls for a modular, distributed approach. However, the infrastructure does not exist and there is limited fundamental insight to convert these four building block molecules into desired traditional feedstocks – such as ethylene – and/or direct commodity chemicals – such as methanol – through low temperature, low energy, low carbon footprint pathways.

Electrochemical schemes are ideal for modular concepts because they scale directly with surface area and current density (not volume), typically operate at low temperature, and are able to achieve efficiencies that are not limited by thermochemical cycles. Also, electrochemical processes provide a unique opportunity to pair with renewable energy sources, such as wind and

solar, which directly produce DC electrons. The cost of these carbon-free electrons has been drastically reduced in the past decade, with the levelized cost of wind and solar being reduced by 66% and 85%, respectively [3], and it is believed that solar and wind electricity may cost less than fossil sources at the grid scale in the next decade. When combined, renewable electricity production and electrochemical synthesis provide a promising low cost ***pathway for completely CO_2-free production of chemicals and fuels***.

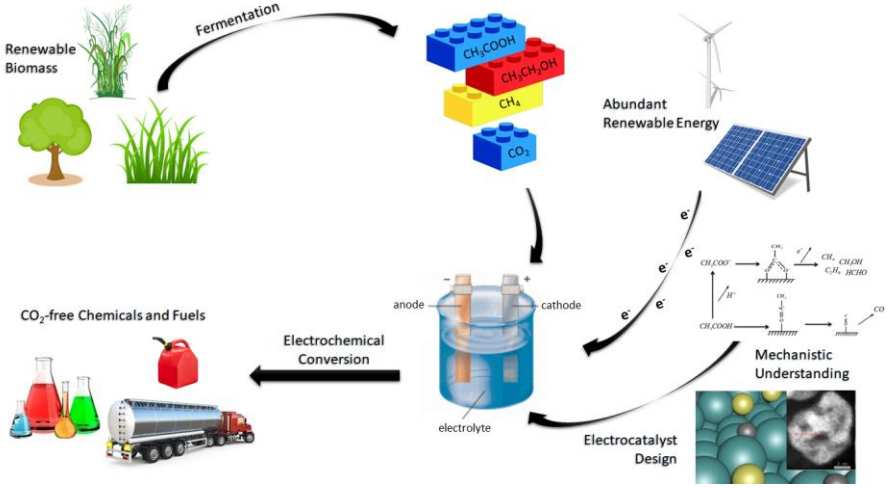

Figure 2. Schematic showing electrochemical conversion of bio-derived CO_2, CH_4, ethanol and acetic acid to value-added products (e.g., paraffins, olefins, methanol) using energy from renewable sources. There is a need for mechanistic understanding and new electrocatalyst design to enable these transformations.

B. Progress with Electrochemical Methane Conversion to Chemicals and Fuels

Methane is one of the most important industrial gases. Not only is it directly used for heat generation, it is the primary feedstock for several of the most widely produced commodity chemicals including hydrogen, ammonia, methanol and formaldehyde. Methane is one of the most widely available resources in the world, with a large amount of it wastefully burned off or vented into the atmosphere. Anthropogenic sources contribute to an estimated 350 million tonnes of methane emissions annually [20]. In the atmosphere methane has 25 times the impact of carbon dioxide on climate change [20]. A primary cause of this waste is difficulty with stable transportation of methane, as well as the heat-intensive process required for methane conversion. A streamlined operation that can convert waste methane to a product more suitable for transportation could turn a pollutant into a revenue generating commodity. Methanol, a primary product of methane conversion, is a very high value product. With a global production capacity around 100 million tonnes per year (demand is ~ 2/3 of capacity), methanol is the world's 5th largest commodity by volume. At a cost of $1.33 a gallon, the methanol industry generates 36 billion dollars in global economic activity and is responsible for 100,000 jobs. Methanol can be used to synthesize numerous products, and has been touted as an important energy carrier of the future. Its high energy density and liquid state in atmospheric conditions make it ideal for stable transportation and storage that is compatible with existing petroleum infrastructure [21-22]. Methane activation and conversion is typically accomplished though syngas production by methane steam reforming which requires high pressure (typically above 10 bar) and high temperature (above 650 ^{o}C). The syngas product is an over oxidized product, necessitating

reduction back to methanol or other desired oxygenates. Although this process is very thermodynamically efficient, the C-H bond has a high dissociation energy requiring a large amount of high quality heat, which comes from burning methane for heat. In fact, over 40% of the methane fed to a syngas reactor is combusted to CO_2. Additionally, the process involves excessive intermediate reaction steps where the methane is over-oxidized to low energy carbon monoxide, and then re-reduced to the higher energy state methanol. This process is inelegant and energetically circuitous, and has potentially unnecessary steps if a high efficiency, direct methane to methanol process can be found.

Since they allow for control of the catalyst surface free energy, electrochemical methods have the potential to reduce the thermal and overall energy barrier to convert methane to oxygenates. However, though noble metal catalysts play a role in the chemical and electrochemical conversion of many chemicals, methane activation on these surfaces has been notoriously difficult. Experiments in strongly acidic media have not yielded any promising candidates to date. We tested an extensive array of transition metal catalysts for the partial oxidation of methane in strongly alkaline media and have found that in traditional potential windows, very little activity, sometimes if any, can be observed. A small portion of our data set using noble metal catalysts in alkaline media for methane activation is shown in Figure 3.

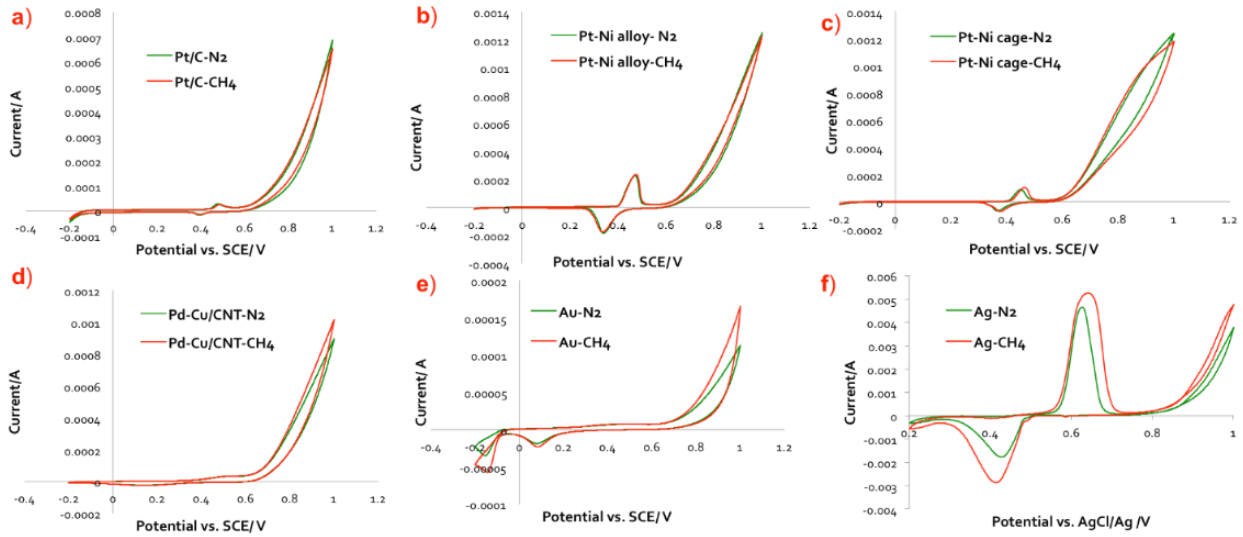

Figure 3. Low methane activation on a wide array of noble metal catalysts in 0.1M KOH electrolyte

Moving forward, we intend to investigate different means to increase the driving force for the reaction including higher potentials, increasing pressure beyond atmospheric pressure and increasing temperature. This is completely unchartered territory and a significant amount of room exists for innovation in this space.

However, it would be advantageous to perform methane oxidation at low potentials since that would directly translate into lower conversion energies – or even the ability to perform these conversions spontaneously at room temperature with an oxygen reduction counter reaction (this could also enable a low temperature direct methane fuel cell, something that has been of great interest for many years). To accomplish this, we believed from our previous work [23-26] that

the redox behavior of surface oxygen in metal oxides, more specifically nickel oxide, could play a role in activating methane. If this were the case, the reaction could proceed by the following proposed mechanism:

In alkaline media, NiO hydrolyzes to $Ni(OH)_2$ and is then oxidized to through an electrochemical surface redox reaction to NiOOH. The reactant, in this case CH_4, approaches the surface, and the reacts with the surface oxygen, returning Ni(III) to Ni(II), Equation 1.

$$NiOOH + CH_4 \rightarrow Ni(II)OH^+ + CH_3OH + e^- \quad (1)$$

The catalyst surface then reacts with OH^- in the electrolyte to form $Ni(OH)_2$, Equation 2, then is re-oxidized to NiOOH electrochemically, Equation 3, where the catalytic cycle begins again.

$$Ni(II)OH^+ + OH^- \rightarrow Ni(OH)_2 + H_2O \quad (2)$$

$$Ni(OH)_2 + OH^- \rightarrow NiOOH + H_2O + e^- \quad (3)$$

Total reaction: $CH_4 + 2OH^- + \rightarrow CH_3OH + H_2O + 2e^-$ (4)

The key intermediate in this proposed mechanism is $Ni(II)OH^+$, which has yet to be identified experimentally, but we would like to use operando XAS measurements in the future to explore the Ni surface state during this reaction as well as the surface state of other transition metal catalysts during methane oxidation. By operating based on such an oxygen insertion mechanism, these methods have the potential to substantially reduce the operating temperature. Processing conditions for electrosynthesis can also be tailored to selectively and dynamically change the reaction selectivity, meaning that the several unit operations that are currently required for the conversion of methane to methanol or formaldehyde might be reduced to a single step. This might be achieved by utilization of a hydroxide/oxyhydroxide couple in hydroxide aqueous media, or by use of a co-catalyst for methane adsorption and oxygen donation from carbonate.

To test a NiO catalyst for methane oxidation, we created a thin-film electrode on an insulated glassy carbon disk. Figure 4a shows cyclic voltammograms for NiO both with and without methane present. In alkaline media, the NiO is immediately hydrolyzed to $Ni(OH)_2$. The reaction that occurs at 0.5 V – 0.6 V vs SCE represents the Ni^{2+}/Ni^{3+} redox couple (Equation 5) to form the electrochemically active NiOOH species shown in Equation 1. The reaction present after 0.85 V vs SCE represents the oxygen evolution reaction (OER, Equation 6).

$$Ni(OH)_2 + OH^- \rightarrow NiOOH + H_2O + e^- \quad (5)$$

$$4OH^- \rightarrow O_2 + 2H_2O + 4e^- \quad (6)$$

This pair of reactions is present both in the absence and presence of methane with no dditional activity under methane saturation. Figure 4c is an EIS IR-corrected Nyquist plot taken at 0.7 V vs SCE, which shows a 37% increase in resistance at the onset of the OER. These combined results indicate that methanol adsorption is occurring, but no activation of methane is taking place on the catalyst surface in this potential window. This confirms the flow cell tests, which showed that the methane formation reactions did not occur until very high potentials, and with low faradaic efficiency due to interference with the OER.

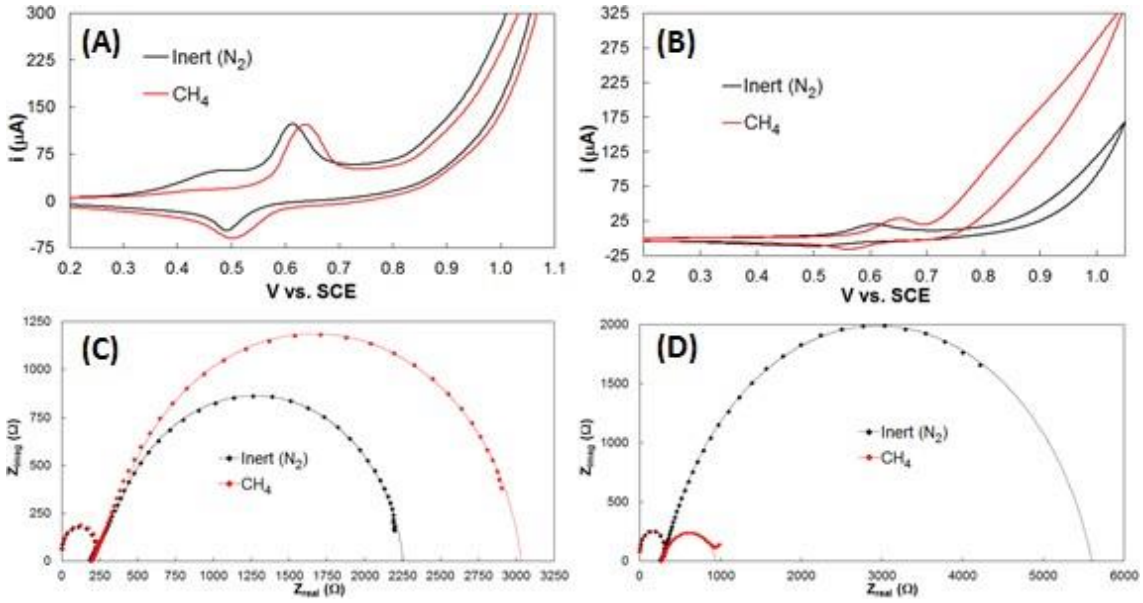

Figure 4. NiO vs NiO:ZrO_2 electrochemical tests in 0.1M Na_2CO_3 electrolyte saturated with nitrogen or methane: Cyclic voltammetry (CV) for NiO (A). CV for NiO:ZrO_2 (B). Electrochemical impedance spectroscopy (EIS) IR-corrected Nyquist plots for NiO (C). EIS IR-corrected Nyquist plots for NiO:ZrO_2 (D).

Zirconia was added to the nickel oxide catalyst for its likely ability to adsorb carbonate ions. The bi-functional catalyst of NiO:ZrO_2 was synthesized using a co-precipitation method, and tested in the same manner as the pure NiO. The CV, shown in Figure 4b, shows a significant increase in activity in carbonate compared to hydroxide. The EIS IR- corrected Nyquist plot for the bi-functional catalyst also showed an 87 % the charge- transfer resistance (Figure 4d.). These tests suggest that the methane is activated on the catalyst using carbonate as an oxygen donor, aiding by adsorption on the ZrO_2 catalyst.

We additionally performed chronoamperometric experiments in flow cells at several voltages for 2 hours each, Figure 5. Figure 5b shows the current draw over the 2 hour period at each voltage. Figure 5c Shows the 1.30 V current vs time data taken on three consecutive days and demonstrates repeatability in the cell. As expected. the current was higher as the voltage increased, though the increase from 1.35 V to 1.40 V and 1.40 V to 1.45 V was much larger than the initial increase from 1.30 V to 1.35 V. Figure 4d shows that this larger increase is likely due to an increase in oxygen evolution in the cell, demonstrated by the sharp decrease in the faradaic efficiency, Figure 5d. This would indicate that an oxygen evolution suppressant may have an impact on the performance of this cell, potentially increasing the faradaic efficiency and the possible operating voltage range. The detection of methanol was also recorded by HPLC and GC/MS. This confirmed the formation of methanol in the cell.

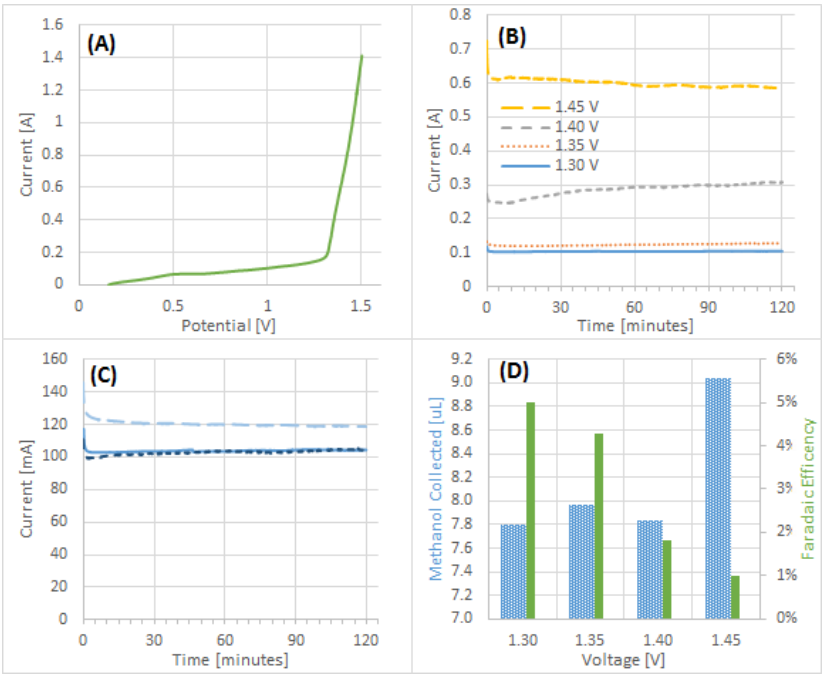

Figure 5. Liquid hydroxide flow cell data: A 2 mV/s linear sweep voltammogram from 0.0 V to 1.5 V (A). Chronoamperometric plots for 2 hour experiments at several voltages (B). Chronoamperometric plots for 2 hours experiments at 1.30 V on 3 consecutive days (C). Methanol collected by hexane cold trap during 2 hour experiments, with faradaic efficiency.

Another interesting note is that methane was primarily activated at moderate pH. This is shown in Figure 6 where data in 0.1 M KOH (Figure 6a) and 0.1 M K_2CO_3 (Figure 6b) can be compared. There was low activity in KOH, but a clear enhancement in carbonate – and several products were detected including CO, HCOH, and CH_3OH (which was the major organic product). Perhaps even more interesting, the nickel oxide catalyst showed photosensitivity where in the presence of even simple room lighting, the redox activity was enhanced in three regions (Figure 5c). At the higher end of the potential window, this is not too surprising since NiOOH is a well-known OER photocatalyst. However, it was surprising that the definition in the Ni(II)→Ni(III) region (~0.55 V vs. Ag/AgCl) was increased since the band edges for $Ni(OH)_2$ and NiOOH make it energetically unfavorable for the holes that may be created in $Ni(OH)_2$, also a semiconductor, to

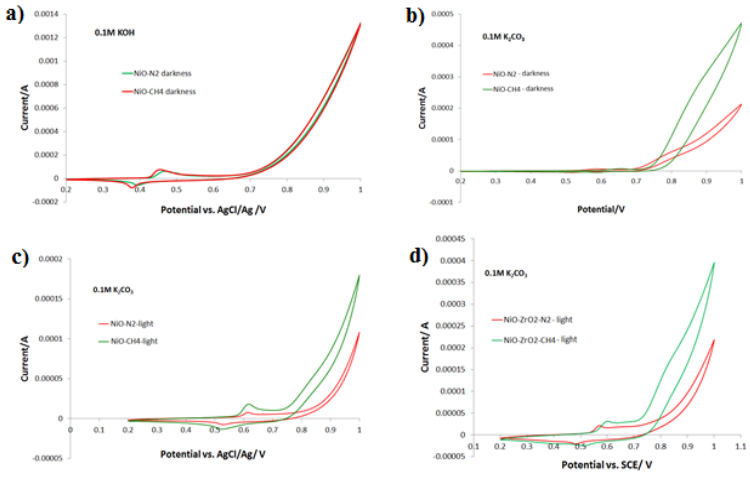

Figure 6. Partial oxidation of methane on NiO-based catalysts. a) NiO in 0.1 M KOH, no light; b) NiO in 0.1 M K_2CO_3, no light; c) NiO in 0.1 M K_2CO_3, open to room light; d) NiO-ZrO_2 co-precipitated catalysts, open to room light.

allow for the formation of NiOOH. Therefore, this enhancement in the Ni hydroxide/oxyhydroxide regime must come from redox activity of NiOOH, requiring addition NiOOH to be produced, which is supported in the potential region between the transition and the OER where a more defined and relatively larger current is observed – suggesting even higher methane activity. Making the picture even more intriguing is that in the presence of co-precipitated ZrO_2 (physically mixing does not work) – which slightly increases the band gap of NiOOH and shifts its band edge – this effect is even further enhanced. This is something that we intend to study further in the future.

C. Acetic Acid Partial Oxidation

During the course of our project, we did design an *operando* electrochemical cell (OEC) that allows our group to quantitatively investigate reaction mechanisms in a realistic reacting environment (Figure 7), while simultaneously allowing for the real-time collection and analysis of products in custom-designed GC and GC/MS systems for differential electrochemical mass spectrometry (DEMS) for gas-phase products as well as NMR and FTIR for liquid phase products during controlled electrochemical experiments.

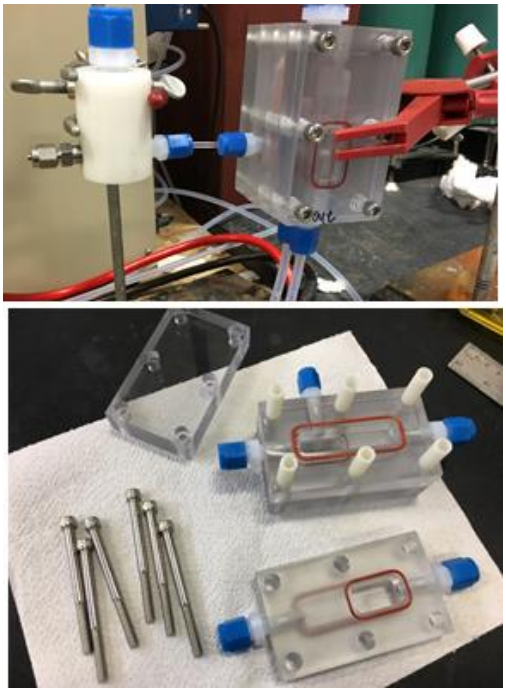

Figure 7. Operando electrochemical cell for GC-DEMS and GC/MS-DEMS experiments – identifying reaction mechanisms for methane and acetic acid oxidation, and other reactions.

Over the course of this project, we investigated several catalysts for the partial oxidation of acetic acid, mostly noble-metal based, including: Pt, PtRu, PtNi nanocages, PtNi alloy, PtCu alloy, and PdCu alloy. A sampling of some of these materials are pictured in Figure 8a. One of our most interesting observation has been that the acetic acid oxidation overpotential is a function of pH. At low (pH~1) and high (pH~13, Figure 8b) pH, acetic acid is oxidized only above the oxygen evolution reaction (OER) potential. However, at intermediate pH, acetic acid oxidation occurs at much lower overpotential, before the OER. This is shown for both Pd-Cu alloy and Pt-Ni nanocages in Figures 4c and 4d, respectively. This atypical behavior suggests, agreeing with Kapalka et al.[27] and Wieckowski et al. [28], that surface water plays an important role in the oxidation mechanism, though at the time of those works there was not widespread access to DFT calculations that are able to quantify the –H, –OH, and $–H_2O$ binding and dissociation energies readily, nor was there an existing concept that these energies may be descriptors for catalytic behavior. This is a link that we will aim to make in the next phase of our work.

The onset of this reaction is accompanied by the emergence of several products including: methanol, methane, formaldehyde, formic acid, ethane, ethylene, methyl formate, methyl acetate

(forming from the reaction of two acetic acid molecules), CO and CO_2 (Figures 9a and 9b). The relationship between the potential and the product distribution is dynamic – and some products only occur at high potentials that have been previously overlooked, which provides a unique opportunity to understand how new pathways emerge with potential and other reaction parameters. For instance, at high potentials, the amount of evolved O_2 decreases, Figure 9a – showing that in at least one preferred pathway an oxygen surface intermediate species is likely needed and/or that the surface is covered more fully with organic intermediates from the increased activity which sterically hinders water from reaching the catalyst surface – both explanations have merit and need to be reconciled. All of the observed discharge products, along with other information from our experiments and the literature have led us to propose an extensive mechanism for the oxidation pathways for acetic acid, Figure 9c – one that may be able to finally explain the complex reaction network and all of the observed products.

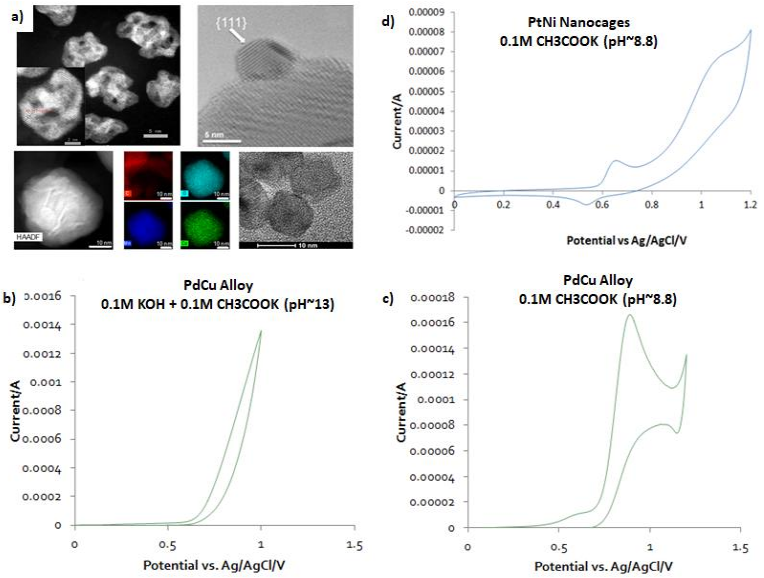

Figure 8. Catalysts and electrochemical response for acetic acid oxidation. a) select catalysts: Pt-Ni nanoframes, Pt on non-C support, MnCoO and NiO:ZrO_2; b) acetic acid oxidation at high pH on Pd-Cu alloy showing no activity other than oxygen evolution; electro-chemical response of c) Pd-Cu alloy and d) Pt-Ni nanocages for acetic acid oxidation at intermediate pH, showing oxidation activity.

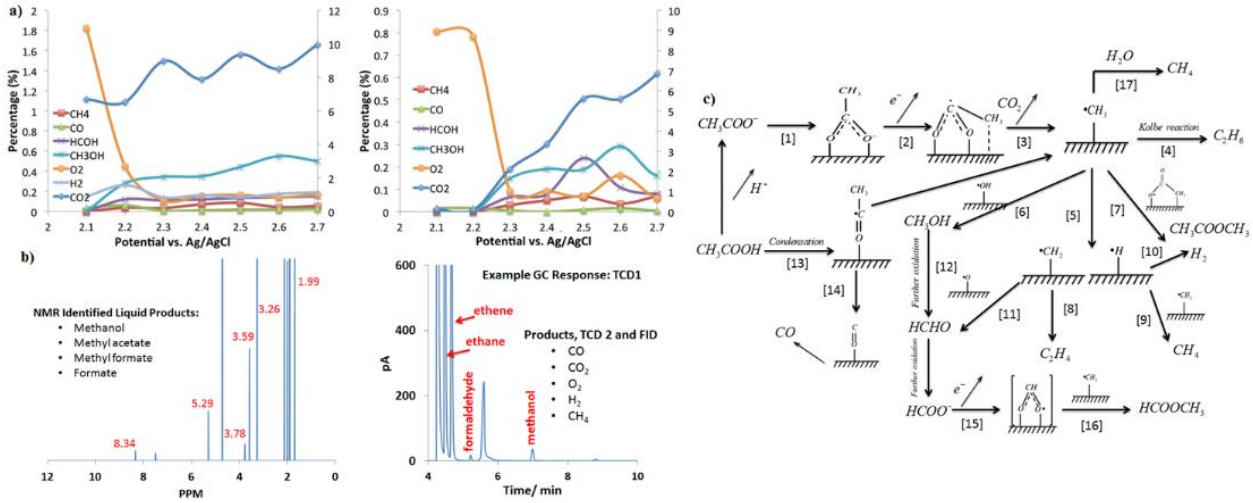

Figure 9. Results from the partial oxidation of acetic acid. a) product profiles as a function of potential and reacting environments; b) example responses from NMR and GC; and c) catalytic pathway proposed by our group.

D. CO_2 Reduction to CO on Preferentially Oriented Ag Electrodes

Of the explored metals for electrochemical reduction of CO_2, gold (Au) and silver (Ag) are reported to have the highest activity and selectivity for CO among the pure transition metals due to their distinctive CO binding energy. Compared to Au, the relatively low cost and higher abundance of Ag makes it a more promising candidate for commercial use. However, a large overpotential is required when using polycrystalline Ag and, though relatively high, the CO faradic efficiency (FE) is still insufficient [29].

In the 1990s, Hori and coworkers studied the orientation and potential dependence of CO_2 electrochemical reduction on Ag single crystal surfaces in order to determine which crystalline facets are the most active [30]. Their results showed that Ag (110) and Ag (100) possess high activity for CO_2 electrochemical reduction to CO. Since then, this has been explained by density functional theory (DFT) calculations have shown that the adsorbed carboxyl (*COOH) was most strongly bound to the Ag (110) facet, followed by Ag (100) and Ag (111), with the Ag (111) surface binding the *COOH the weakest [32]. However, translating their findings to producing highly active and selective nanoparticles has been elusive to date. Therefore, the overarching goal of this work was to produce a preferentially-oriented Ag electrocatalyst (PON-Ag) with low index preferential faceting in order to achieve the elusive combination of very high catalyst activity and very high faradaic efficiency.

The PON-Ag catalyst was synthesized by electro-anodization/reduction cycles with an Ag foil in 0.5 M $KHCO_3$. The anodization treatment created a layer of Ag_2CO_3 (Figure 10a) on the electrode surface, which was subsequently reduced to Ag nanoparticles (Figure 10b) and then used for CO_2 electrochemical reduction. After reduction, the OD-Ag exhibits a much rougher surface with uniformly distributed particles (Figure 10c,d) and average thickness of 2.5 μm (Figure 10e). Bicarbonate electrolyte was used with the intention of first oxidizing Ag to Ag_2CO_3 because it was believed that the rapid destruction of the monoclinic structure (in the subsequent electro-reduction) and recombination of Ag would result in more (100) and (110) surface orientation than the same process from cubic Ag_2O. In addition to the preferential faceting, the method used in this study has another advantage over other

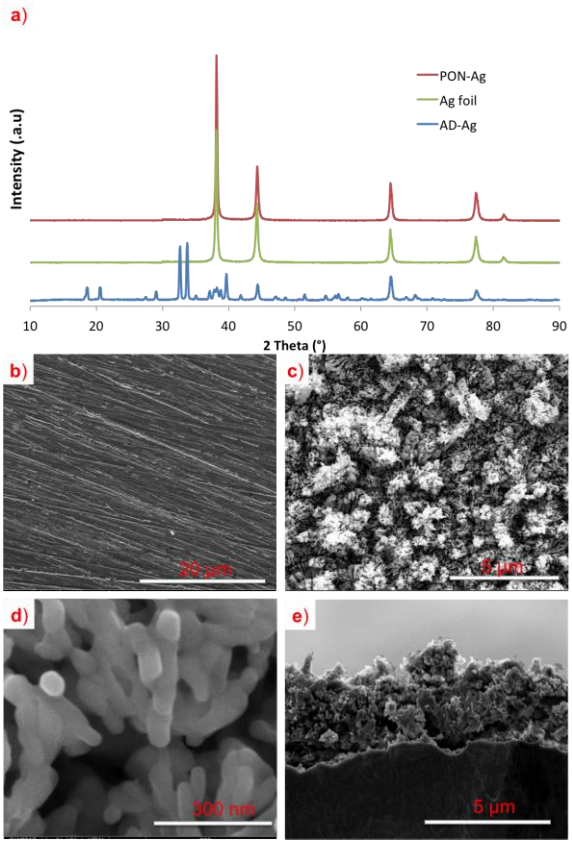

Figure 10. (a) XRD patterns of Ag_2CO_3, PON-Ag and polycrystalline Ag-foil; Representative SEM images of (b) Ag foil surface; (c) (d) (e) OD-Ag

existing approaches in that it does not require different electrolytes to conduct the anodization treatment and to perform CO_2 reduction, which avoids introducing impurities and possible detachment of the oxidized Ag particles when changing the electrolyte for subsequent CO_2 electrolysis. This electrode fabrication method is also simple and scalable, and may even allow for in-situ catalyst regeneration or self-healing, and which will be probed in future work

The electrochemical reduction of CO_2 was investigated on PON-Ag [32] and two primary gas-phase products were found: CO and H_2. The PON-Ag showed very high rates and CO selectivity. Figure 11a presents iR-corrected total reduction current densities (normalized to the geometric electrode area) as a function of potential, which were measured chronoamperometrically.

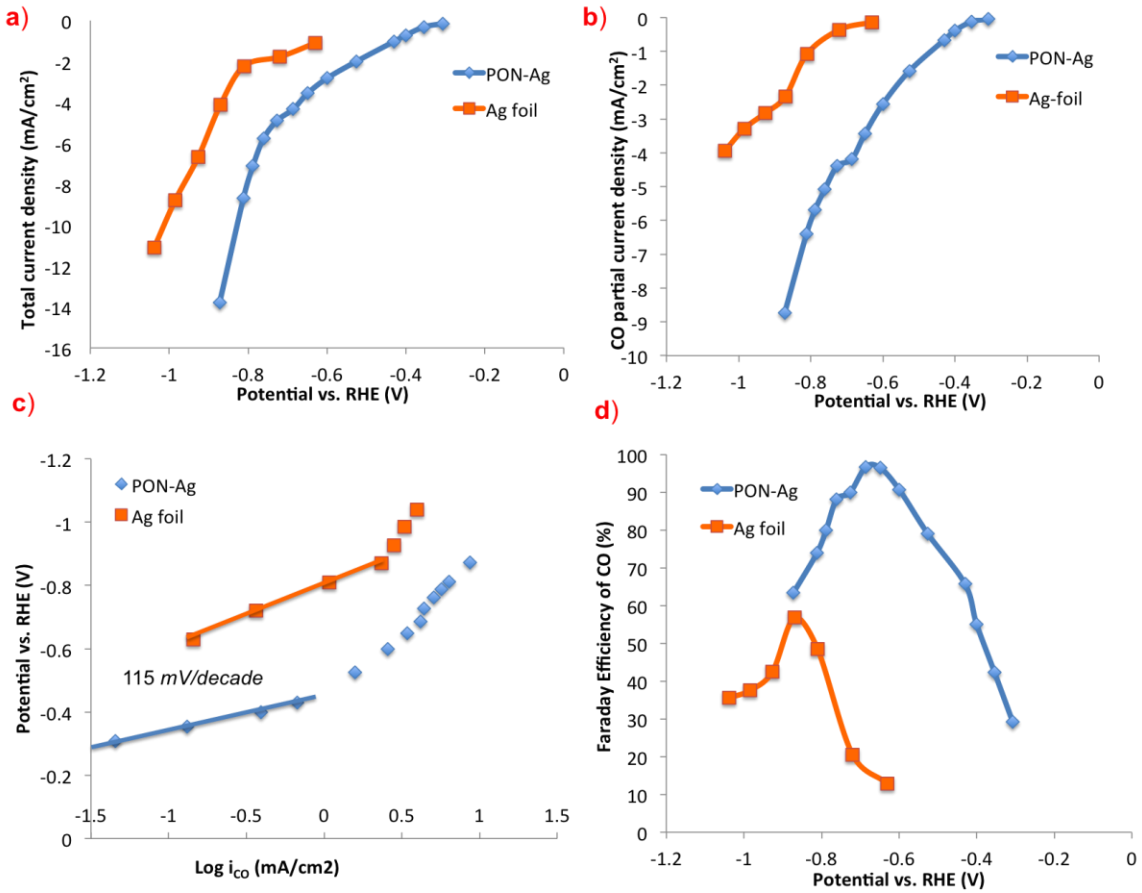

Figure 11. Electrochemical characterization of polycrystalline Ag foil and PON-Ag electrodes showing: (a) total reduction current density; (b) CO partial current density as a function of potential (iR-corrected); (c) Tafel plot of overpotential as a function of CO partial current density; and (d) CO faradaic efficiency as a function of potential (current densities normalized by geometric surface area).

The PON-Ag showed a much higher total reduction current density than the Ag foil, at least partly because of the enhanced surface area. From this data, the CO partial current density was calculated, and the result is plotted in Figure 11b. The PON-Ag showed a higher CO partial current density than that of the polycrystalline Ag at all operating potentials, ranking the second

highest among all of the materials reported in the literature to date. One of the most significant results of this work is that the onset potential for CO_2 reduction on PON-Ag was high, meaning low overpotential, where a measureable CO partial current density (> -0.05 mA/cm^2) was found at only 0.3 *V vs.* RHE (0.19 V overpotential). It should be noted that the polycrystalline Ag had a much lower cathodic onset potential (higher reaction overpotential), matching well with previous literature.

In order to gain kinetic insights into the enhanced catalytic activity of CO_2 reduction to CO on PON-Ag from the electrochemical data, Tafel plots (potential *vs.* log of the partial current density) were created and are shown in Figure 11c. The PON-Ag electrode showed a Tafel slope of 115 mV/decade for CO production, which suggests that the surface formation of a surface adsorbed *COOH intermediate is the rate-determining step [32].

The selectivity for CO_2 reduction to CO was also investigated on the PON-Ag and polycrystalline Ag electrodes and is represented by plotting the CO faradaic efficiency (FE_{CO}) as a function of the operating potential in Figure 11d. Both PON-Ag and Ag foil showed a volcano-like potential dependence for FE_{CO}. The PON-Ag showed enhanced CO selectivity over the hydrogen evolution reaction at lower reaction overpotential than the polycrystalline Ag electrode. In addition, the maximum CO faradaic efficiency was 96.7% at an operating potential of -0.69 *V* (0.58 V overpotential), which was much higher than that of the polycrystalline Ag foil (60% at -0.87 *V*). It is also interesting to note that although the CO faradaic efficiency decreased from -0.72 to -0.9 *V vs.* RHE, the CO partial current density continued increasing in this potential range, indicating that the decrease in CO selectivity was not due to a decrease in the CO production rate, but a more rapidly increasing production rate for H_2 because of its high exchange current density. Moreover, the CO_2 electrochemical reduction activity and selectivity of PON-Ag electrodes prepared in the work were compared with other top-performing silver-based electrocatalysts – with a very attractive combination of low overpotential, high partial current density and high faradaic efficiency.

Finally, the stability of the PON-Ag electrodes for CO_2 electrochemical reduction was examined continuously over a two 2-hour period (7 injections) at each potential. Even over two hours of operation, the PON-Ag electrode showed very good stability. For instance, the PON-Ag was able to achieve a CO_{FE} of 87% at an operating potential of -0.72 V vs. RHE, which was very similar to the initial performance data shown in Figure 11d. Also, the measured current and Tafel slope did not appreciably decline during the test – showing that the PON-Ag catalyst not only achieved very high performance, but excellent stability as well.

E. Synergistic Advances Realized Through This DOE Funded Project

As discussed in the sections above many new discoveries have been made during the course of this project related to catalysis generally, and electrocatalysis specifically. However, it is also worth reporting that this work was not done in a bubble – and our efforts enabled to cross-cutting advances in other fields. For instance, our methane activation work on NiO led us to question how NiO would behave in non-aqueous electrolytes. In the past few years, we have made

advances in understanding how NiO conversion reactions (with Li^+) store charge; this project led to one publication where this grant is acknowledged [33] as well as additional papers on NiO [34-35] and other redox-active metal oxides [36-39] that were the result of funding by Ford Motor Company based on our initial results related to this project.

Another example where this project has led to interesting results in other fields is that the attempt to scaleup methanol production from methane in alkaline media led us to explore multiple pathways to create porous electrodes. Not only did we make new electrode structures for methane activation, but they were also highly efficient for proton exchange membrane fuel cells [40-41] and anion exchange membrane fuel cells [42-43]. In fact, in the anion exchange membrane fuel cell field, our group has set new records in the literature for achievable current and power. Finally, our work in this project in alkaline media – specifically in the presence of CO_2 and carbonates – led to the discovery that anion exchange systems could also be used to extract CO_2 from effluent streams, and we were able to propose a new electrochemical reactor for the capture of carbon dioxide from power plants [44]. For full details on each of these processes, please see the referenced papers.

F. Products

F.1 Peer Reviewed Publications

1. N. Spinner and W.E. Mustain, "Electrochemical Methane Activation and Conversion to Oxygenates at Room Temperature", J. Electrochem. Soc., 160 (2013) F1275-F1281.
2. T.J. Omasta, W.A. Rigdon, C.A. Lewis, R.J. Stanis, R. Liu. C.Q. Fan and W.E. Mustain, "Two Pathways for Near Room Temperature Electrochemical Conversion of Methane to Methanol", ECS Trans., 66(8) (2015) 129-136
3. S.D. Poynton, R.T.C. Slade, T.J. Omasta, W.E. Mustain, R. Escudero-Cid, P. Ocon, and J.R. Varcoe, "Preparation of radiation-grafted powders for use as anion exchange ionomers in alkaline polymer electrolyte fuel cells", J. Mat. Chem. A., 2 (2014) 5124-5130.
4. N.S. Spinner, A. Palmieri, N. Beauregard, L. Zhang, J. Campanella and W.E. Mustain, "Influence of Conductivity on the Capacity Retention of NiO Anodes in Li-ion Batteries", J. Power Sources, 276 (2015) 46-53.
5. W.A. Rigdon, T.A. Omasta, C.A. Lewis and W.E. Mustain, "Reaction Dependent Transport of Carbonate and Bicarbonate through Anion Exchange Membranes in Electrolysis and Fuel Cell Operations", ECS Trans. 69(33) (2015) 1-9.
6. W.A. Rigdon, T.J. Omasta, C. Lewis, M. Hickner, J.R. Varcoe, J.N. Renner, K.A. Ayers and W.E. Mustain, "Carbonate dynamics and opportunities with low temperature, AEM-based electrochemical CO_2 separators", *J. Electrochem. En. Conv. Stor.*, 12(2) (2017), 020901
7. X. Peng, S. Zhao, T. Omasta, J.M. Roller and WE. Mustain, "Activity and durability of Pt-Ni nanocage electocatalysts in proton exchange membrane fuel cells", *Applied Catalysis B: Environmental*, 203 (2017) 927-935.

8. X. Peng, T.J. Omasta, W. Rigdon and W.E. Mustain, "Fabrication of high performing PEMFC catalyst-coated membranes with a low cost air-assisted cylindrical liquid jets spraying system", *J. Electrochem. Soc.*, 163 (2016) E407-E413.
9. X. Peng, T.J. Omasta, J.M. Roller and W.E. Mustain, "Highly active and durable Pd-Cu catalysts for oxygen reduction in alkaline exchange membrane fuel cells", *Frontiers in Energy*, 11 (2017) 299-309
10. T.J. Omasta, L. Wang, X. Peng, C.A. Lewis, J.R. Varcoe and W.E. Mustain, "Importance of Balancing Membrane and Electrode Water in Anion Exchange Membrane Fuel Cells", *J. Power Sources*, 375 (2018) 205-213. DOI: 10.1016/j.jpowsour.2017.05.006.
11. X. Peng, S.G. Karakalos and W.E. Mustain, "Preferentially oriented Ag nanocrystals with extremely high activity and faradaic efficiency for CO_2 electrochemical reduction to CO", *ACS Applied Materials and Interfaces*, Accepted – In Press; DOI: 10.1021/acsami.7b16164.
12. T. J. Omasta, A. M. Park, J. M. LaManna, Y. Zhang, X. Peng, L. Wang, D. L. Jacobson, J. R. Varcoe, D. S. Hussey, B. S. Pivovarc and W. E. Mustaina, "Beyond Catalysis and Membranes: Visualizing and Solving the Electrode Water Challenge in AEMFCs", Submitted for Review
13. X. Peng, T.J. Omasta, S.G. Karakalos and W.E. Mustain, "Electrochemical Pathways for Electrochemical Oxidation of Acetic Acid", In Preparation

F.2 Invited Presentations

1. "Termite-Inspired Electrochemical Processing of Lignocellulose to Chemicals and Fuels", AIChE Annual Meeting, Minneapolis, MN, October 2017.
2. "Advances in Electrocatalysis of Fuels and Anion Exchange Membrane Fuel Cells – Inspired by Termites?", Department of Chemical and Biomolecular Engineering, Case Western Reserve University, September 2017.
3. "Understanding Water and Ion Transport in ETFE-based Membranes and Ionomers in Operating Anion Exchange Membrane Fuel Cells", 21st International Conference on Solid-State Ionics, Padua, Italy, June 2017.
4. "Importance of Carbonates in the Low Temperature Electrochemical CO_2 Cycle and New Opportunities", Beijing Forum 2016 on Electrochemical Frontier – Alkaline Membrane Fuel Cells: Catalysts and Materials. Wuhan, China, December 2016.
5. "An Electrochemical Approach for CO_2 Capture from Fossil Fuel Power Plants", D Nora Research Symposium, De Nora Global R&D Headquarters, November 2016.
6. "Improvements in the Anion Exchange Membrane Transport of Carbonate and Bicarbonate for Low-Temperature CO_2 Capture and Energy Conversion", 230th Meeting of Electrochemical Society, October 2016.
7. "An Electrochemical Approach for CO_2 Capture from Fossil Fuel Power Plants", US-UK Fulbright Commission, Endcap Event, Glasgow, Scotland, UK, June 2016.
8. "An Electrochemical Approach for CO_2 Capture from Fossil Fuel Power Plants", Department of Chemical Engineering, Imperial College London, UK, June 2016.

9. "An Electrochemical Approach for CO_2 Capture from Fossil Fuel Power Plants", Department of Chemical and Process Engineering, University of Surrey, UK, June 2016.36.
10. "Advanced Carbonate Exchange Membrane Electrochemical Cells to Reduce CO_2 Emissions", School of Chemical Engineering & Advanced Materials, Newcastle University, UK, May 2016.
11. "Near Room Temperature Electrochemical Methane to Methanol Electrosynthesis", Department of Chemistry, University of Surrey, UK, May 2016.
12. "Importance of Carbonates in the Low Temperature Electrochemical CO_2 Cycle and New Opportunities", Department of Chemical Engineering, University of South Carolina, February 2016.
13. "Importance of Carbonates in the Low Temperature Electrochemical CO_2 Cycle and New Opportunities", Department of Chemical & Biological Engineering, Colorado School of Mines, February 2016.
14. "Importance of Carbonates in the Low Temperature Electrochemical CO_2 Cycle and New Opportunities", National Renewable Energy Laboratory, February 2016.
15. "Low Temperature Electrochemical Upgrading of Methane to Methanol", AIChE Annual Meeting, Salt Lake City, UT, November 2015.
16. "Near Room Temperature Electrochemical Upgrading of Methane to Oxygenate Fuels", DOE Catalysis Science Program Meeting, Annapolis, MD, July 2015.
17. "Carbonates and Low Temperature Electrochemical Systems", Electrochemical Tutorials Session, AIChE National Meeting, November 2014.
18. "Innovative Catalyst Design for Energy Conversion", Connecticut Quality Improvement Award Parnership, 27th Annual Conference on Quality and Innovation, June 2014.
19. "Purposeful Utilization of Carbonate Anions in AEM-Based Devices", 7th Santa Fe Workshop on Materials for Energy Conversion, Bishop's Lodge, Santa Fe, NM, November 2013.

Additionally, there have been over 30 presentations at professional conferences (not listed here).

G. References Cited

1. M. Weiss, M.K. Patel, M. Junginger, A. Perujo, P. Bonnel and G. van Grootveld, "On the electrification of road transport - Learning rates and price forecasts for hybrid-electric and battery-electric vehicles", *Energy Policy*, 48 (2012) 374-393.
2. A. Boulanger, A.C. Chu, S. Maxx and D.L. Waltz, "Vehicle Electrification: Status and Issues", *Proceedings of the IEEE*, 99 (2011) 1116-1138.
3. LAZARD's Levelized Cost of Energy Analysis, Version 10.0, Dec. 2016. https://www.lazard.com/media/438038/levelized-cost-of-energy-v100.pdf
4. U.S. Global Change Resarch Program, "Climate Science Special Report: Fourth National Climate Assessment (NCA4), Volume I", 2017. https://science2017.globalchange.gov/
5. B. Gardiner, "The Paris agreement really does change everything", The Guardian online edition, October 7, 2016. https://www.theguardian.com/commentisfree/2016/oct/07/paris-agreement-climate-change-carbon-emissions
6. S. Nadal, N. Elliott and T. Langer, "Energy Efficiency in the United States: 35 Years and Counting", American Council for an Energy-Efficient Economy, Report E1502, 2015.
7. Lawrence Livermore National Laboratory, "Estimated U.S. Energy Consumption in 2016", https://flowcharts.llnl.gov/content/assets/images/energy/us/Energy_US_2016.png
8. U.S. Energy Information Administration, "Energy Use in Industry", https://www.eia.gov/energyexplained/index.cfm?page=us_energy_industry
9. D.H.R. Barton, "The Invention of Chemical Reactions", *Aldrichimica Acta*, 23 (1990) 3.
10. Special Issue of Accounts of Chemical Research. *Acc. Chem. Res.* Vol 28 (1995), 91-162
11. R.A. Himes and K.D. Karlin, "A New Copper-oxo Player in Methane Activation", *Proc. Nat. Acad. Sci. USA*, 106 (2009) 18877.
12. U.S. Department of Energy, "Basic Research Needs: Catalysis for Energy", 2007.
13. International Energy Agency, "Tracking Industrial Energy Efficiency and CO_2 Emissions", 2007. https://www.iea.org/publications/freepublications/publication/tracking_emissions.pdf
14. International Energy Agency, "Chemical and Petrochemical Sector: Potential of best practice technology and other measures for improving energy efficiency", 2009. https://www.iea.org/publications/freepublications/publication/chemical_petrochemical_sector.pdf
15. U.S. Department of Energy Office of Science, "Basic Research Needs for Clean and Efficient Combustion of 21st Century Transportation Fuels", 2006.
16. U.S. Department of Energy Office of Science, "New Science for a Secure and Sustainable Energy Future", 2008.
17. R. Cho, "Is Biomass Really Renewable?", State of the Planet. August 18, 2011. http://blogs.ei.columbia.edu/2011/08/18/is-biomass-really-renewable/
18. U.S. Department of Energy, "2016 Billion Ton Report: Advancing Domestic Resources for a Thriving Bioeconomy, Volume 1", 2016.

19. U.S. Department of Energy, Energy Efficiency and Renewable Energy, "Regional Feedstock Partnership Summary Report: Enabling the Million Ton Vision", July 2016. https://www.energy.gov/sites/prod/files/2016/07/f33/regional_feedstock_partnership_summary_report.pdf
20. S. Menon, K. L. Denman, G. Brasseur, A. Chidthaisong, P. Ciais, P. M. Cox, R. E. Dickinson, D. Hauglustaine, C. Heinze, E. Holland, D. Jacob, U. Lohmann, S. Ramachandran, Leite da Silva Dias, Pedro, S. C. Wofsy and X. Zhang, in Climate Change 2007 – The Physical Science Basis: Contribution of Working Group I to the Fourth Assessment Report of the IPCC, S. Solomon, Editor, p. 498, Cambridge University Press, 2007 (2007)
21. G. A. Olah, A. Goeppert and S. K. Surya-Prakash, Beyond oil and gas: the methanol economy, Wiley-VCH (2009).
22. G. A. Olah, "Beyond oil and gas: the methanol economy", *Angew Chem Int Ed.*, 44, (2005) 18.
23. N. Spinner and W.E. Mustain, "Electrochemical Methane Activation and Conversion to Oxygenates at Room Temperature", *J. Electrochem. Soc.*, 160(11) (2013) F1275-1281.
24. N. Spinner and W.E. Mustain, "Electrochemical Methane Activation and Conversion to Oxygenates at Room Temperature", *ECS Trans.*, 53(23) (2013) 1-20.
25. N. Spinner and W.E. Mustain, "Effect of Nickel Oxide Synthesis Conditions on its Physical Properties and Electrocatalytic Oxidation of Methanol", *Electrochimica Acta*, 56 (2011) 5656
26. N. Spinner and W.E. Mustain, "Influence of non-conducting zirconia on the electrochemical performance of nickel oxide in alkaline media at room temperature", *J. Electrochem. Soc.*, 159 (2012) E187.
27. A. Kapalka, G. Foti and C. Comninellis, "Investigation of the Anodic Oxidation of Acetic Acid on Boron-Doped Diamond Electrodes", *J. Electrochem. Soc.*, 155 (2008) E27-E32.
28. A. Wieckowski, J. Sobrowski and P. Zelenay, "Adsorption of acetic acid on platinum, gold and rhodium electrodes" *Electrochimica Acta*, 26 (1981) 1111-1119.
29. Hatsukade, T.; Kuhl, K. P.; Cave, E. R.; Abram, D. N.; Jaramillo, T. F. Insights into the Electrocatalytic Reduction of CO2 on Metallic Silver Surfaces. Phys.Chem.Chem.Phys 2014, 16 (27), 13814–13819.
30. Hoshi, N.; Kato, M.; Hori, Y. Electrochemical Reduction of CO on Single Crystal Electrodes of Silver. J. Electroanal. Chem. 1997, 440, 283–286.
31. Back, S.; Yeom, M. S.; Jung, Y. Active Sites of Au and Ag Nanoparticle Catalysts for CO 2 Electroreduction to CO. ACS Catal. 2015, 5, 5089–5096.
32. X. Peng, S.G. Karakalos and W.E. Mustain, "Preferentially oriented Ag nanocrystals with extremely high activity and faradaic efficiency for CO_2 electrochemical reduction to CO", *ACS Applied Materials and Interfaces*, Accepted – In Press; DOI: 10.1021/acsami.7b16164.

33. N.S. Spinner, A. Palmieri, N. Beauregard, L. Zhang, J. Campanella and W.E. Mustain, "Influence of Conductivity on the Capacity Retention of NiO Anodes in Li-ion Batteries", J. Power Sources, 276 (2015) 46-53
34. N. Spinner, L. Zhang and W.E. Mustain, "Investigation of Nickel Oxide Anode Degradation in Lithium-ion Batteries via Identical-Location TEM", *J. Mat. Chem. A*, 2(6) (2014) 1627-1630.
35. A. Palmieri, T. Wang, J. Zhang, N. Spinner, M. Liu and W.E. Mustain, "Modeling Nickel Oxide Particle Stress Behavior Induced by Lithiation Using a FEM Linear Elastic Approach", *J. Electrochem. Soc.*, 164 (2017) A867-A873. DOI: 10.1149/2.1501704jes
36. S. Yazdani, R. Sabadad, A. Palmieri, W.E. Mustain and M. Pettes, "Effect of cobalt alloying on the electrochemical performance of manganese oxide nanoparticles nucleated on multiwalled carbon nanotubes", *Nanotechnology*, 28 (2017) 115403.
37. A. Palmieri, R. Kashfi-Sadabad, S. Yazdani, M. Pettes and W.E. Mustain, "High Performance Bi-Metallic Manganese Cobalt Oxide/Carbon Nanotube Li-ion Battery Anodes", *Electrochimica Acta*, 213 (2016) 620-625.
38. J. He, Y. Liu, Y. Meng, X. Sun, S. Biswas, M. Shen, Z. Luo, R. Miao, L. Zhang, W.E. Mustain and S.L. Suib, "High-rate and long-life of Li-ion batteries using reduced graphene oxide/Co_3O_4 as anode materials", RSC Advances, 6 (2016) 24320-24330.
39. Y. Liu, A. Palmieri, J. He, Y. Meng, N. Beauregard, S.L. Suib and W.E. Mustain, "Highly Conductive In-SnO_2/RGO Nano-Heterostructures with Improved Lithium-Ion Battery Performance", *Scientific Reports*, 6 (2016) 25860; doi: 10.1038/srep25860.
40. X. Peng, S. Zhao, T. Omasta, J.M. Roller and WE. Mustain, "Activity and durability of Pt-Ni nanocage electocatalysts in proton exchange membrane fuel cells", *Applied Catalysis B: Environmental*, 203 (2017) 927-935.
41. X. Peng, T.J. Omasta, W. Rigdon and W.E. Mustain, "Fabrication of high performing PEMFC catalyst-coated membranes with a low cost air-assisted cylindrical liquid jets spraying system", *J. Electrochem. Soc.*, 163 (2016) E407-E413.
42. X. Peng, T.J. Omasta, J.M. Roller and W.E. Mustain, "Highly active and durable Pd-Cu catalysts for oxygen reduction in alkaline exchange membrane fuel cells", *Frontiers in Energy*, 11 (2017) 299-309
43. T.J. Omasta, L. Wang, X. Peng, C.A. Lewis, J.R. Varcoe and W.E. Mustain, "Importance of Balancing Membrane and Electrode Water in Anion Exchange Membrane Fuel Cells", *J. Power Sources*, 375 (2018) 205-213. DOI: 10.1016/j.jpowsour.2017.05.006.
44. W.A. Rigdon, T.J. Omasta, C. Lewis, M. Hickner, J.R. Varcoe, J.N. Renner, K.A. Ayers and W.E. Mustain, "Carbonate dynamics and opportunities with low temperature, AEM-based electrochemical CO_2 separators", *J. Electrochem. En. Conv. Stor.*, 12(2) (2017), 020901